Contact Resistance Properties of Cold-Pressing Superconducting Joints

Junsheng Cheng, Lankai Li, Feng Zhou, Jianhua Liu, Chunyan Cui, Xinning Hu, Yinming Dai, Luguang Yan, Shunzhong Cheng, and Yi Li

***Abstract*—A NbTi superconducting joint technology applied for MRI/NMR has been developed with a cold-pressing method. The plastic deformation microstructure of the fabricated joint was investigated by using scanning electron microscopy and optical microscope. The joint resistances were tested using coil current decay method. The contact resistance properties of the superconducting joint were investigated. The evolution of plastic deforming and the electrical contact characteristics of the NbTi superconducting joint are discussed. It is believed that the contact resistance is composed of constriction resistance and film resistance. With the pressure increasing, the dominant factor is changed from the film resistance to the constriction resistance. Finally, the joint resistance is inversely proportional to the cubic root of applied pressure. The joint resistance correlates with the increase in plastic deformation with increased pressure.**

***Index Terms*—Cold-pressing, contact resistance, plastic deformation, superconducting joint.**

I. Introduction

RECENTLY a series of superconducting magnets with the characteristics of high homogeneity and high stability were constructed in our laboratory, including the 400 MHz superconducting nuclear magnetic resonance spectrometer (NMR) magnet [1] and the 9.4 T large bore magnetic resonance imaging (MRI) magnet [2], [3]. For MRI/NMR measurements, field stability higher than ~0.1 ppm/h is required. To achieve this, the main coils of the magnet are joined in series with superconducting joints and the magnets are operated in persistent mode. Field stability of a magnet depends on the resistance in the coil circuit and inductance. The total resistance in the circuit is equal to the summation of wire resistance in each coil and joint. The superconducting wire resistances can be ignored in case there is a considerable current margin in the magnet design. The contribution from joint resistance is basically a summation of resistances of all interconnections in the circuit. To achieve satisfactory magnetic field stability in the MRI/NMR system, the joints between magnet and its switch, and those between different sections of the magnet must be made with great care. It is necessary that the resistance of the superconducting joints should be extremely low for the persistent current decay.

There are three mainly methods to make the NbTi multifilamentary wire joints; they are cold-pressing, solder welding and diffusion bonding. Among them, solder welding is commonly used [4], [5]. However, both the non-uniformity of solder and temperature error will affect the joint quality. Especially, it is difficult to prevent surface oxidation during heating. As to the diffusion bonding method [6], the vacuum condition in fabrication process limits its application. Comparatively the cold-pressing method is convenient and reliable. The mechanism of cold-pressing joint is complicated. Theory and technology of cold-pressing joint fabrication should be intensively studied. However few presentations on this can be found in publications. Recently the preliminary numerical simulation and electrical properties studies on cold-pressing joint technologies have being done by Wang *et al.* [7], [8]. In this paper, contact resistance properties of the cold-pressing superconducting joint were farther studied by discussing the plastic deforming evolution and the electrical contact characteristics.

Manuscript received August 11, 2014; accepted November 5, 2014. Date of publication November 20, 2014; date of current version January 20, 2015. This work was supported in part by the National Natural Science Foundation of China under Grant 11155001, Grant 51107135, and Grant 51477167, and by the National Major Scientific Equipment R&D Project under Grant ZDYZ2010-2.

The authors are with the Institute of Electrical Engineering and the Key Laboratory, Applied Superconductors, Chinese Academy of Sciences, Beijing 100190, China (e-mail: jscheng@mail.iee.ac.cn).

Color versions of one or more of the figures in this paper are available online at http://ieeexplore.ieee.org.

Digital Object Identifier 10.1109/TASC.2014.2370097

II. Experimental

A. Joint Fabrication

A type of NbTi/Cu multifilament superconducting wire was chosen for the cold-pressing joint experiment. The diameter of the wire is 0.5 mm. The NbTi alloy filament number is 54. The filament diameter is about 10 micron. The ratio of copper to superconductor is 1.3.

A kind of NbTi/Cu composite tube was introduced in the cold-pressing method jointing procedure. A layer of 99.99% pure copper is located on the cylindrical surface of NbTi alloy tube. The internal layer is NbTi superconducting alloy. The purpose of the copper layer is to prove heat transfer and reduce the electrical resistance.

The supporting die of the pressing machine is made of tool steel. To increase pressure stability, there is an angle of 1–2° between the upper and the lower dies.

The cold-pressing joint was fabricated under open air condition using a hydraulic machine. Its pressure range is up to 60 ton.

The cold-pressing joint fabrication process includes five steps.

Step 1) Remove the copper matrix of the wire by nitric acid until only a brush-like bundle of NbTi filaments was left;

Step 2) Clean and dry the filaments;

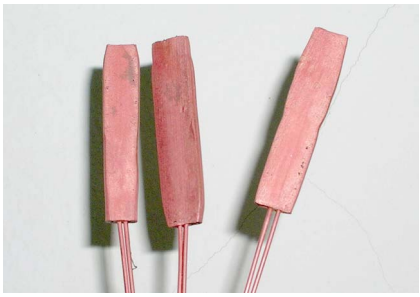

Fig. 1. Configuration of some joints made by cold-pressing method.

Step 3) Insert the filaments into NbTi/Cu composite tube;
Step 4) Place the tube together with filaments into the gap between the two supporting dies of a hydraulic machine;
Step 5) Press the joint. During this step, the NbTi filaments are embedded in the composite tube to form the joint.

Some of the joints we made are shown in Fig. 1.

B. Testing and Apparatus

The morphology and the microstructure of the joint were studied by ZEISS ULTRA 55 field-emission scanning electron microscope (SEM) and optical microscope (OM). The boundary layer thickness and the space counts of the joints were obtained using the image analysis software.

Generally, the MRI/NMR magnetic field decay is less than 0.05–0.1 ppm/h [9], [10]. The resistance of the individual joint should be no more than 0.01 nano-ohm [11]. The resistance of joint sample was measured by coil current decay method. This method is to measure the decay of the magnetic field produced by the current induced in a superconducting loop which includes a joint.

The test system, which consists of a current transformer, a bias field magnet, a cryogenic Hall probe and a small loop to be tested, had been set up [12]–[14]. An AMI power supply with nominal maximum output current of 200 Amp (model 12200PS-420) was used to charge the bias magnet and the current transformer. The cryogenic Hall probe is from Lakeshore (model HGCA-3020). Voltage taps across the Hall sensor was connected to a Keithley model 2000 Multimeter, which then transferred the voltage data to a PC based system using LabView software through an IEEE- 88 bus.

III. Results and Discussion

A. Evolution of Deformation of Filaments During Pressing

There are several different mold shapes to choose in cold-pressing joint fabrication: plate mold, cap mold, square mold, and radial compression mode [8], [13], [14]. To study the effect of pressing process on the joint plastic deformation and resistance evolution, the simple plate mold was adopted in this paper. To study the evolution characters of the joints after pressure deforming, several joint samples were fabricated under different pressure values, from 520 to 1150 MPa [10].

The optical microscope micrographs of the cross section of the joints are shown separately in Fig. 2. To observe the morphology of the samples clearly, the cross-sections were polished and etched.

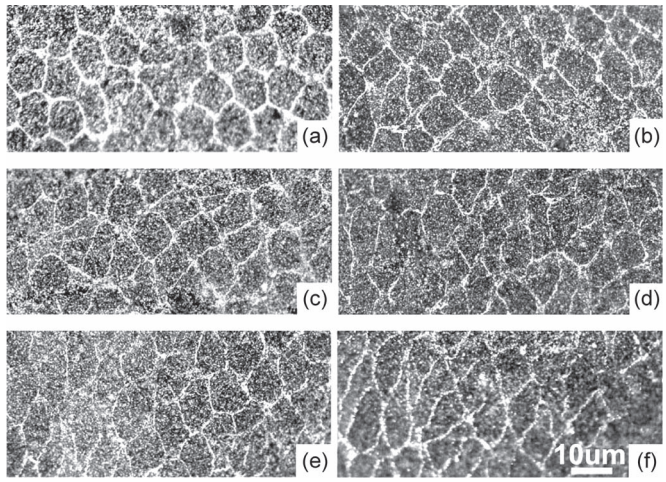

Fig. 2. OM images of NbTi filaments in the joints by various pressure conditions. (a) 520 MPa; (b) 650 MPa; (c) 820 MPa; (d) 990 MPa; (e) 1040 MPa; (f) 1150 MPa.

From the micrograph of the cross-section of the 520 MPa sample we can see that plastic deformation has happened in the NbTi filaments. But the plastic deformation looks so slight that the boundary thickness of the filaments looks very broad. The even value of the boundary thickness reaches 0.5 micron. It means that the boundary bonding is not stable enough. Also the round cross section of the filaments only changed to hexagon. These hexagon deformed filaments still kept the equiaxed features. There are still some spaces between the filaments, shown as the white dots in the micrograph. It can be calculated that the space area is about 1.2% of the cross-section. And the size of the largest space reaches 1.3 micron in diameter. It is noticeable that the white dots all appeared in the triangle intersection area among adjacent three filaments. Obviously the triangle intersection area is the weakness of the filament deformation and would affect the contact area ratio. As a whole, it seems that the sample under 520 MPa pressure loads has so little plastic deform that some surfaces between the filaments still do not contact tightly. It shows that the 520 MPa pressure is too low for the joint.

In the second micrograph of Fig. 2, the pressure load was raised to 650 MPa. It shows that most of filaments in the joint still keep the equiaxed features. However the most remarkable characteristic of the sample is that the number of white dots reduced considerably. The percentage of the total area of space is reduced to about 0.7%. Also the thickness of boundary between the filaments has been decreased to $0.1 \sim 0.2$ micron. It implies that the interface bonding of NbTi filament was stronger than the former sample.

When the pressure value increased to 820 MPa, the boundary thickness of the filaments reduced continually to about 0.1 micron. Also a majority of filament cross sections changed shape from round to approximate ellipse. This implies that there was not any space in the joint and the bonding process between the filaments had been completed under this cold press condition.

With the pressure continually increasing to 990, 1040 and 1150 MPa, we could find that the boundary thickness of the

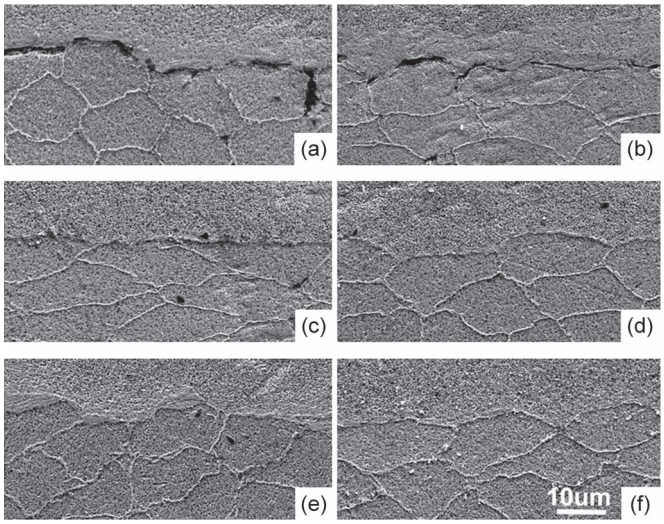

Fig. 3. SEM images of bonding morphologies between the NbTi filament and the tube under different pressure conditions. (a) 520 MPa; (b) 650 MPa; (c) 820 MPa; (d) 990 MPa; (e) 1040 MPa; (f) 1150 MPa.

filaments remains a constant small value. The only change is the ellipse cross section become more and more flat. The ratio of the major axis to short axis increases from one to two roughly.

B. Bonding Between Filament and Tube

The plastic deformation evolution between the filament and the tube is also studied. The bonding morphologies between the filament and the tube under different pressure conditions are shown in Fig. 3.

It can be seen from Fig. 3 that there exists a gap between filaments and the tube in the 520 MPa sample. When the pressure increased to 650 MPa, the width of the gap decreased obviously. A few cold weld bonding in the sample was found. When the pressure increased to 820 MPa, cold weld bonding formed in most areas except a few spaces at the boundary. When the pressure was increased to 990 MPa, the space in the sample were completed disappeared, as shown in Fig. 3(d). Also there is no space found in the two samples with the higher pressure, as shown in Fig. 3(e) and (f). The severe plastic deformation of the materials contributes to the increased contact area and better surface bonding.

In summary, at the beginning of the joint plastic deformation, the space between the filaments is filled up and the contact area increases with the increase of pressure. After then, the contact area enhances continually by the ellipse cross section becoming more and more flat with the increase in pressure. The above mentioned mechanical evolution strongly influences the electrical contact characteristics.

C. Contact Resistance of the Joint

The joint resistance comes from the electrical contact of interface of the joint by cold pressing. There are two types of the electrical contact in the joint. One is the contact among the filaments; the other is the contact between the filament and the tube. According to electrical contact theory [10], contact resistance is the resistance to current flow, due to surface conditions and other causes, when two solid surfaces are touching each other. Contact resistance, R_k, is defined as the sum of the constriction resistance, R_E, and the film resistance, R_F, as the following equation [15],

$$\mathrm{R}_k = \mathrm{R}_\mathrm{E} + \mathrm{R}_F. \tag{1}$$

The constriction resistance caused by the decreased contact area is due to the imperfect contact of the two bodies at the interface. In the cold-pressing joint, the actual contact areas are smaller than the surface areas of the filaments. The constriction resistance is expressed as [15],

$$\mathrm{R}_\mathrm{E} = \frac{\rho}{\pi \mathrm{r}_\mathrm{k}} \tag{2}$$

where, ρ is the resistivity of NbTi alloy, r_k is the diameter of the contact area. Under conditions of severe plastic deformation, the diameter of the contact area is expressed as [15],

$$\mathrm{r}_k = \sqrt[3]{\frac{F_k}{\pi H}} \tag{3}$$

where, H is the hardness, F_k is the contact pressure.

From (2), it could be seen that the constriction resistance of the joint directly is inversely proportional to the diameter of the contact area. So, to reduce constriction resistance, the contact area should be increased. Equation (3) shows that the contact pressure is directly proportional to the cubic of the diameter of the contact area assuming the hardness is constant. From the two equations, it may be deduced that the constriction resistance of the joint is inversely proportional to the cubic root of contact pressure.

The film resistance is caused by the resistive film covered on the contact surface. If the film is produced only by physical sorption of gas molecule on the contact surface, the film breaks down during severe plastic deformation. In this deformation condition, the film resistance may be ignored. However, if the gas molecule is chemically combined with the metal molecule to form an inorganic film, such as an oxide, nitride and sulfide, the film resistance of the film must be considered. The film resistance, R_F, is expressed as [15],

$$\mathrm{R}_\mathrm{F} = \frac{\rho_\mathrm{F}\mathrm{d}}{\pi \mathrm{r}_\mathrm{k}^2} \tag{4}$$

where, ρ_F is the film resistivity, d is the thickness of the film. Combined with the above equations, the contact resistance may be expressed as [15],

$$\mathrm{R}_k = \frac{\rho}{\pi \mathrm{r}_\mathrm{k}} + \frac{\rho_\mathrm{F}\mathrm{d}}{\pi \mathrm{r}_\mathrm{k}^2}. \tag{5}$$

Assuming the film resistivity is constant, Equation (5) may be simplified as [15],

$$\mathrm{R}_k = K F_k^{-m} \tag{6}$$

where, K is a constant value, m is a coefficient with the range of 0.33 to 3, or larger. The value of coefficient corresponds to the severity of the film destruction. The more seriously the film is broken, the larger the coefficient is.

Equation (6) may be converted to (7) by applying logarithm function on both sides,

$$\ln(\mathrm{R}_k) = \ln K - m \ln(F_k) \tag{7}$$

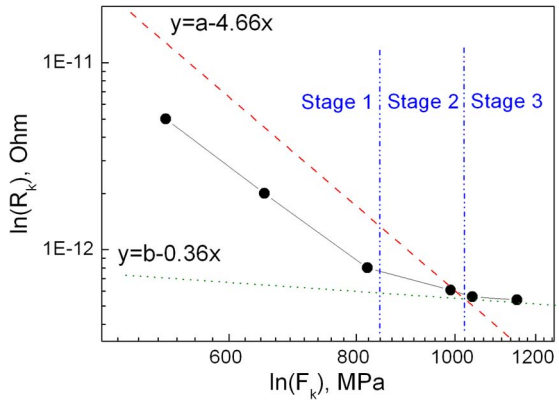

Fig. 4. Pressure dependence of the joint resistance.

From (7), it is clear that the coefficient m is the slope of the fitted curve of $\ln(F_k)$ vs. $\ln(R_k)$.

To validate the relationship between contact resistance and contact pressure mentioned above, the resistances of series joint samples with various pressures were measured in liquid helium temperature. The joints resistances are shown in Fig. 4. It can be seen that the joint has the resistance of less than 10^{-12} Ohm which is acceptable for persistent operation. It is clear that the resistance of the joint is reduced at a declining rate with the increase of pressure.

To obtain the value of the coefficient m, the curve of logarithmic pressure vs. logarithmic resistance of the joints was fitted in Fig. 4. The coefficient m is determined by the slope of the curve. According to the slope-change trend, there are three stages of the decreasing resistance.

During the first stage, the joint resistance decreased linearly form 5×10^{-12} Ohm at the 520 MPa pressure to 8×10^{-13} Ohm at the 820 MPa pressure. The fitted linear expression is shown in Fig. 4. The slope of the fitted line is 4.66. Then the coefficient m, as high as 4.66, indicates that the film is broken seriously under the applied force.

In the second stage, the reducing rate of the joint resistance is much lower than that of the first stage. The reduced slope indicates the smaller coefficient. It means that the broken effect of the film was weakened. At this pressure, the role of the constriction resistance is increased.

In the last stage, the coefficient is reduced to 0.36, closing to the minimum value of 0.33. It indicates that the effect of the film is almost insignificant. At this pressure, the joint resistance is dominated by the constriction resistance.

The evolution of plastic deformation mostly matches the reduction of joint resistance with the increase of pressure. At the beginning of the cold-pressing, the filaments and the tube are pressed together tightly. As pressure is increased, the boundary of the filament becomes narrowed, the space is reduced, and the film is broken gradually. In the first stage, the sharp decline in resistance attributed to the film resistance plays a major role. In the second stage, with the increased pressure, the effect of the constriction resistance is enhanced compared with the film resistance. In this stage, most of the filaments and tube have been cold welded together. In the last stage, both the space and film are disappeared wholly. The severe plastic deformation of the materials contributes to the increased contact area and better surface bonding. In this stage, the constriction resistance is the only factor of the contact resistance, and the film resistance may be ignored. Summarily, the joint cold-pressing process can be divided into three stages as above mentioned: film resistance stage, combined resistance stage and constriction resistance stage.

IV. Conclusion

The contact resistance properties of the superconducting joint by cold-pressing method were investigated. The plastic deforming process and the electrical contact characteristics of the NbTi superconducting joint were discussed. It is believed that the cold-pressing joint resistance comes from the contact resistance. The contact resistance is composed of the constriction resistance and the film resistance. With the pressure increasing, the joint cold-pressing process can be divided into three stages: film resistance stage, combined resistance stage and constriction resistance stage. Finally, the joint resistance is inversely proportional to the cubic root of applied pressure. The joint resistance correlates with the plastic deformation which is increasing with the increase of the pressure.

References

[1] Q. Wang *et al.*, "High magnetic field superconducting magnet for 400 MHz nuclear magnetic resonance spectrometer," *IEEE Trans. Appl. Supercond.*, vol. 21, no. 3, pp. 2072–2075, Jun. 2011.
[2] Y. Dai *et al.*, "Structural design of a 9.4 T whole-body MRI superconducting magnet," *IEEE Trans. Appl. Supercond.*, vol. 22, no. 3, Jun. 2012, Art. ID. 4900404.
[3] Q. Wang, *Practical Design of Magnetostatic Structure Using Numerical Simulation*. Singapore: Wiley, 2013.
[4] S. Liu *et al.*, "Superconducting joint and persistent current switch for a 7-T animal MRI magnet," *IEEE Trans. Appl. Supercond.*, vol. 23, no. 3, Jun. 2013, Art. ID. 4400504.
[5] C. A. Swenson and W. D. Markiewicz, "Persistent joint development for high field NMR," *IEEE Trans. Appl. Supercond.*, vol. 9, no. 2, pp. 185–188, Jun. 1999.
[6] H. Wen, L. Lin, and S. Han, "Joint resistance measurement using current-comparator for superconducting wires in high magnetic field," *IEEE Trans. Magn.*, vol. 28, no. 1, pp. 834–836, Jan. 1992.
[7] J. Liu, J. Cheng, and Q. Wang, "Evaluation of NbTi superconducting joints for 400 MHz NMR magnet," *IEEE Trans. Appl. Supercond.*, vol. 23, no. 6, Dec. 2013, Art. ID. 4802606.
[8] F. Zhou *et al.*, "Numerical simulation of mold shape's influence on NbTi cold-pressing superconducting joint," *Physica C, Supercond.*, vol. 498, pp. 9–13, Mar. 2014.
[9] J. Liu *et al.*, "Electrical properties of cold-pressing welded NbTi persistent joints," *Cryogenics*, vol. 58, pp. 62–67, Dec. 2013.
[10] F. Zhou *et al.*, "Numerical simulation of NbTi superconducting joint with cold-pressing welding technology," *IEEE Trans. Appl. Supercond.*, vol. 23, no. 6, Dec. 2013, Art. ID. 4802706.
[11] Y. Lvovsky, E. W. Stautner, and T. Zhang, "Novel technologies and configurations of superconducting magnets for MRI," *Supercond. Sci. Technol.*, vol. 26, no. Sep. 2013, Art. ID. 093001.
[12] J. Cheng *et al.*, "Fabrication of NbTi superconducting joints for 400-MHz NMR," *IEEE Trans. Appl. Supercond.*, vol. 22, no. 2, Apr. 2012, Art. ID. 4300205.
[13] Q. Wang, L. Yan, B. Zhao, and S. Song, "Development of wide-bore conduction-cooled superconducting magnet system for material processing applications," *IEEE Trans. Appl. Supercond.*, vol. 14, no. 2, pp. 372–375, Jun. 2004.
[14] Q. Wang *et al.*, "Open MRI magnet with iron rings correcting the lorentz force and field quality," *IEEE Trans. Appl. Supercond.*, vol. 24, no. 3, Jun. 2014, Art. ID. 4402305.
[15] H. Hoft and H. G. Schnerder, *Electrical Contact*. Berlin, Germany: Akademie-Verlag, 1980.